

Pairing interactions and pairing mechanism in high temperature copper oxide superconductors

G uo-m eng Zhao

Department of Physics and Astronomy, California State University, Los Angeles, CA 90032, USA

The polaron binding energy E_p in undoped parent cuprates has been determined to be about 1.0 eV from the unconventional oxygen-isotope effect on the antiferromagnetic ordering temperature. The deduced value of E_p is in quantitative agreement with that estimated from independent optical data and that estimated theoretically from the measured dielectric constants. The substantial oxygen-isotope effect on the in-plane supercarrier mass observed in optimally doped cuprates suggests that polarons are bounded into the Cooper pairs. We also identify the phonon modes that are strongly coupled to conduction electrons from the angle-resolved photoemission spectroscopy, tunneling spectra, and optical data. We consistently find a very strong electron-phonon coupling feature at a phonon energy of about 20 m eV along the antinodal direction. On the other hand, the coupling to the 20 m eV phonon mode becomes weaker towards the diagonal direction so that the coupling features at higher phonon energies become more pronounced. We further show that high-temperature superconductivity in cuprates is caused by strong electron-phonon coupling, polaronic effect, and significant coupling with 2 eV Cu-O charge transfer fluctuation.

I. INTRODUCTION

Developing the microscopic theory for high- T_c superconductivity is one of the most challenging problems in condensed matter physics. Eighteen years after the discovery of the high- T_c cuprate superconductors by Bednorz and Müller¹, there have been no microscopic theories that can describe the physics of high- T_c superconductors completely and unambiguously. Due to the high T_c values and the observation of a small oxygen-isotope effect in a 90 K cuprate superconductor $\text{YBa}_2\text{Cu}_3\text{O}_{7-y}$ (YBCO)³, many theorists believe that the electron-phonon interaction is not important in bringing about high- T_c superconductivity. Most physicists have thus turned their minds towards alternative pairing interactions of purely electronic origin.

On the other hand, there is overwhelming evidence that electron-phonon coupling is very strong in cuprates⁵⁻¹⁹. In particular, the studies of various unconventional oxygen-isotope effects Zhao and his coworkers have initiated since 1992 clearly indicate that the electron-phonon interactions are so strong that polarons/bipolarons are formed in doped cuprates and manganites^{5-9,11-16,18,20}, in agreement with a theory of high-temperature superconductivity²¹. However, such clear experimental evidence for strong electron-phonon interactions from the unconventional isotope effects has been generally ignored. In the 2001 Nature paper¹⁷, Lanzara et al. appear to provide evidence for a strong coupling between doped holes and the 70 m eV half-breathing phonon mode from angle-resolved photoemission spectroscopy (ARPES). They further show that this 70 m eV phonon mode can lead to d-wave pairing symmetry and is mainly responsible for high-temperature

superconductivity²². Very recently, Dereux et al.²³ have proposed that the 40 m eV B_{1g} phonon mode rather than 70 m eV half-breathing phonon mode is responsible for d-wave high-temperature superconductivity. This pairing mechanism contradicts the very recent ARPES data from their own group, which show that multiple phonon modes at 27 m eV, 45 m eV, 61 m eV, and 75 m eV are strongly coupled to doped holes in deeply underdoped $\text{La}_{2-x}\text{Sr}_x\text{CuO}_4$ ¹⁹. The strong coupling to the multiple phonon modes is not in favor of d-wave gap symmetry but may support a general s-wave gap symmetry^{24,25}.

Here we determine the polaron binding energy E_p for undoped parent cuprates from the unconventional oxygen-isotope effect on the antiferromagnetic ordering temperature (T_N)⁵. The determined value (1.0 eV) of E_p is in quantitative agreement with that estimated from independent optical data²⁶ and that estimated theoretically from the measured dielectric constants²⁷. The substantial oxygen-isotope effect on the in-plane supercarrier mass observed in optimally doped cuprates^{6,16,18} indicates that polarons are bounded into the Cooper pairs. We also identify the phonon modes that are strongly coupled to conduction electrons from the angle-resolved photoemission spectroscopy, tunneling spectra, and optical data. We consistently find a very strong electron-phonon coupling feature at a phonon energy of about 20 m eV along the antinodal direction. On the other hand, the coupling to the 20 m eV phonon mode becomes weaker towards the diagonal direction so that the coupling features at higher phonon energies become more pronounced. We further show that high-temperature superconductivity in cuprates is caused by strong electron-phonon coupling, polaronic effect, and significant coupling with 2 eV Cu-O charge transfer fluctuation.

II. OXYGEN-ISO TOPE EFFECT ON T_N IN La_2CuO_4

The antiferromagnetic order (AF) observed in the parent insulating compounds like La_2CuO_4 signals a strong electron-electron Coulomb correlation. On the other hand, if there is a very strong electron-phonon coupling such that the Migdal adiabatic approximation breaks down, one might expect that the antiferromagnetic exchange energy should depend on the isotope mass. Following this simple argument, Zhao and his co-workers initiated studies of the oxygen isotope effect on the AF ordering temperature in several parent compounds in 1992. A noticeable oxygen-isotope shift of T_N was consistently observed in La_2CuO_4 ⁵.

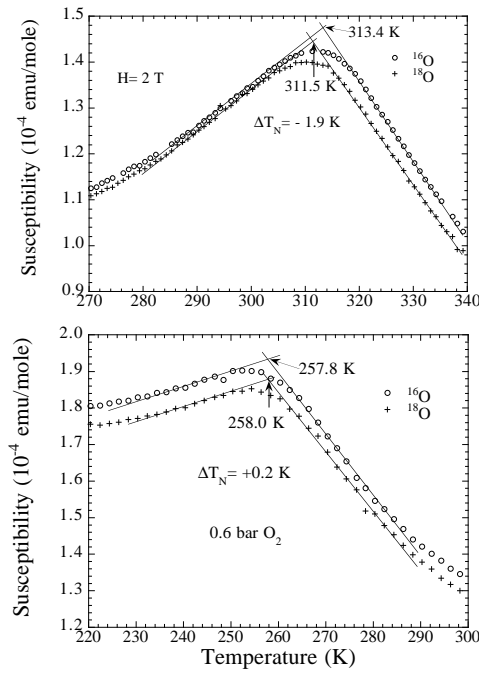


FIG. 1. The temperature dependence of the susceptibility for the ^{16}O and ^{18}O samples of undoped La_2CuO_4 (upper panel), and of the oxygen-doped $\text{La}_2\text{CuO}_{4+y}$ (lower panel). After⁵.

Fig. 1 shows the temperature dependence of the susceptibility for the ^{16}O and ^{18}O samples of undoped La_2CuO_4 (upper panel), and of oxygen-doped $\text{La}_2\text{CuO}_{4+y}$ (lower panel). One can see that the AF ordering temperature T_N for the ^{18}O sample is lower than the ^{16}O sample by about 1.9 K in the case of the undoped samples. For the oxygen-doped samples, there is a negligible isotope effect.

It is known that the antiferromagnetic properties of $\text{La}_2\text{CuO}_{4+y}$ can be well understood within mean-field theory which leads to a T_N formula²⁸:

$$k_B T_N = J^0 [(T_N) = a]^2; \quad (1)$$

where J^0 is the interlayer coupling energy, (T_N) is the in-plane AF correlation length at T_N with $(T_N) / \exp(J=T_N)$ for $y=0$ (J is the in-plane exchange energy). When T_N is reduced to about 250 K by oxygen doping, a mesoscopic phase separation has taken place so that $(T_N) = L$ (Ref.²⁹), where L is the size of the antiferromagnetically correlated clusters, and depends only on the extra oxygen content y . In this case, we have $T_N = J^0(L=a)^2$. Since L is independent of the isotope mass, a negligible isotope shift of T_N in the oxygen-doped $\text{La}_2\text{CuO}_{4+y}$ suggests that J^0 is independent of the isotope mass. Then we easily find for undoped compounds

$$T_N = T_N = (J=J) \frac{B}{1+B}; \quad (2)$$

where $B = 2J=T_N \approx 10$. From the measured isotope shift of T_N for the undoped samples, we obtain $J=J \approx 0.6\%$.

Recently, Erem et al.³⁰ have considered strong electron-phonon coupling within a three-band Hubbard model. They showed that the antiferromagnetic exchange energy J depends on the polaron binding energy E_p^O due to oxygen vibrations, on the polaron binding energy E_p^{Cu} due to copper vibrations, and on their respective vibration frequencies ω_o and ω_{Cu} . At low temperatures, J is given by³⁰

$$J = J \left(1 + \frac{3E_p^O h \omega_o}{2 \omega_{pd}} + \frac{3E_p^{Cu} h \omega_{Cu}}{2 \omega_{pd}} \right); \quad (3)$$

Here ω_{pd} is the charge-transfer gap, which is measured to be about 1.5 eV in undoped cuprates. The oxygen-isotope effect on J can be readily deduced from Eq. 3:

$$\frac{J}{J} = \left(\frac{3E_p^O h \omega_o}{2 \omega_{pd}} \right) \left(\frac{\omega_{pd}}{\omega_o} \right); \quad (4)$$

Substituting the unbiased parameters $\hbar \omega_o = 0.075$ eV, $J=J \approx 0.6\%$, $\omega_{pd} = 1.5$ eV, and $\omega_{pd}/\omega_o = 6.0\%$ into Eq. 4, we find that $E_p^O = 1.0$ eV. The total polaron binding energy should be larger than 1.0 eV since E_p^{Cu} should not be zero. The parameter-free estimate of the polaron binding energy due to the long-range Fröhlich-type electron-phonon interaction has been made for many oxides including cuprates and manganites²⁷. The total polaron binding energy for La_2CuO_4 was estimated to be about 1 eV, in excellent agreement with the value deduced above from the isotope effect. The polaron binding energy can be also estimated from optical data where the energy of the mid-infrared peak in the optical conductivity is equal to $2 E_p$ (Ref.²⁷), where E_p is between 0.2-0.3 (Ref.²⁷). The peak position ($2 E_p$) was found to be about 0.6 eV for $\text{La}_{1.97}\text{Sr}_{0.03}\text{CuO}_4$ (Ref.²⁶), implying that $E_p = 1.0-1.5$ eV. This is in quantitative agreement

with the value estimated from the isotope effect. These results thus consistently suggest that the polaron binding energy of undoped La_2CuO_4 is about 1 eV. Doping will reduce the value of E_p due to screening. For the optimal doping ($x = 0.15$), the optical data suggest that $2 E_p = 0.12$ eV, which is a factor of 5 smaller than that for $x = 0.03$.

III. OXYGEN-ISOTOPE EFFECT ON THE IN-PLANE SUPERCARRIER MASS

One of the most remarkable oxygen-isotope effects we have observed is the oxygen-isotope effect on the penetration depth^{6,9,13,16,18}. We made the first observation of this effect in optimally doped $\text{YBa}_2\text{Cu}_3\text{O}_{6.93}$ in 1994⁶. By precisely measuring the diamagnetic signals for the ^{16}O and ^{18}O samples, we were able to deduce the oxygen-isotope effects on the penetration depth (δ) and on the supercarrier density n_s . It turns out that $n_s \neq 0$, and $\delta(0) = \delta(0) = 3.2\%$ (Ref. ⁶). These isotope effects thus suggest that the effective supercarrier mass depends on the oxygen-isotope mass.

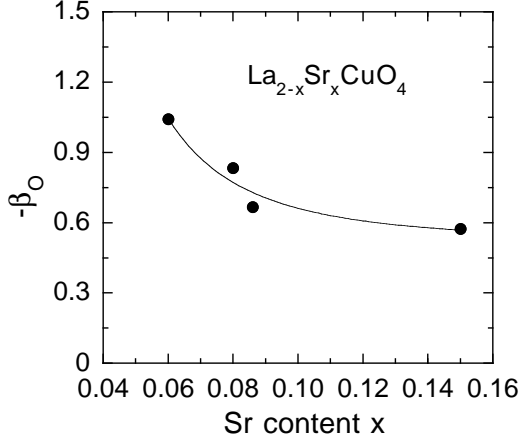


FIG. 2. The doping dependence of the exponent (α) of the oxygen-isotope effect on the in-plane supercarrier mass in $\text{La}_{2-x}\text{Sr}_x\text{CuO}_4$. The exponent is defined as $\alpha = d \ln m_{ab} = d \ln M_0$. The data are from Ref.^{13,15,16}.

In fact, for highly anisotropic materials, the observed isotope effect on the angle-averaged (δ) is the same as the isotope effect on the in-plane penetration depth (δ_{ab}). From the magnetic data for $\text{YBa}_2\text{Cu}_3\text{O}_{6.93}$, $\text{La}_{1.85}\text{Sr}_{0.15}\text{CuO}_4$, and $\text{Bi}_{1.6}\text{Pb}_{0.4}\text{Sr}_2\text{Ca}_2\text{Cu}_{10+y}$, we found that $\delta_{ab}(0) = \delta_{ab}(0) = 3.2 \pm 0.7\%$ for the three optimally doped cuprates¹⁶. Several independent experiments have consistently shown that the carrier densities of the two isotope samples are the same within 0.0004 per unit cell^{8,9,14}. Therefore, we can safely conclude that the observed oxygen-isotope effect on the in-plane

penetration depth is caused only by the isotope dependence of the in-plane supercarrier mass. Recently, direct measurements of the in-plane penetration depth by low energy muon-spin-relaxation (LESR) technique¹⁸ have confirmed our earlier isotope effect results. It was found that¹⁸ $\delta_{ab}(0) = \delta_{ab}(0) = 2.8 \pm 1.0\%$. It is remarkable that the isotope effect obtained from the most advanced and expensive technology (LESR) is the same as that deduced from simple magnetic measurements.

Fig. 2 shows the doping dependence of the exponent (α) of the oxygen-isotope effect on the in-plane supercarrier mass in $\text{La}_{2-x}\text{Sr}_x\text{CuO}_4$. Here the exponent is defined as $\alpha = d \ln m_{ab} = d \ln M_0$. It is apparent that the exponent increases with decreasing doping, in agreement with the fact that doping reduces electron-phonon coupling due to screening. The large oxygen-isotope effect on the in-plane supercarrier mass cannot be explained within the conventional phonon-mediated pairing mechanism where the effective mass of supercarriers is independent of the isotope mass³¹. In particular, the substantial oxygen-isotope effect on m_{ab} in optimally doped cuprates indicates that the polaronic effect is not vanished in the optimal doping regime where the BCS-like superconducting transition occurs. This suggests that polaronic carriers may be bounded into the Cooper pairs in optimally doped and overdoped cuprates.

IV. STRONG ELECTRON-PHONON COUPLING FEATURES ALONG THE DIAGONAL DIRECTION

In conventional superconductors, strong electron-phonon coupling features can be identified from single-particle tunneling spectra. For high- T_c cuprates, high-quality tunneling spectra are difficult to obtain because of a short coherence length. Moreover, due to a strong gap anisotropy, the energies of the strong coupling features will depend on the tunneling directions. Only if one can make a directional tunneling, one may be able to identify the electron-phonon coupling features from the tunneling spectrum. On the other hand, the observation of the electron self-energy renormalization effect in the form of a "kink" in the band dispersion may reveal coupling of electrons with phonon modes. The "kink" feature at an energy of about 65 meV has been seen in the band dispersion of various cuprate superconductors along the diagonal ("nodal") direction¹⁷. From the measured dispersion, one can extract the real part of electron self-energy that contains information about coupling of electrons with collective boson modes. The energy of a broad peak in the electron self-energy should correspond to the averaged energy of all the bosonic modes that couple to electrons if the superconducting gap is zero along the diagonal direction. The fine coupling structures can be only revealed in the high-resolution ARPES data. Very recently, such fine coupling structures have been clearly

seen in the raw data of electron self-energy of deeply underdoped $\text{La}_{2-x}\text{Sr}_x\text{CuO}_4$ along the diagonal direction¹⁹. Using the maximum entropy method (MEM) procedure, they are able to extract the electron-phonon spectral density ${}^2\text{F}(!)$ that contains coupling features at 27 meV, 45 meV, 61 meV and 75 meV. These beautiful ARPES data and exclusive data analysis¹⁹ clearly indicate that the phonons rather than the magnetic collective mode are responsible for the electron self-energy effect.

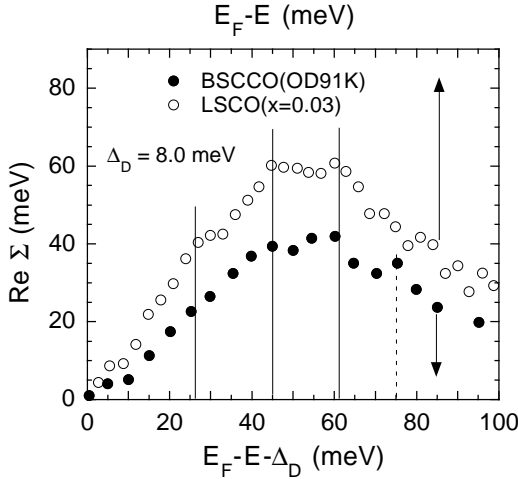


FIG. 3. The real part of electron self-energy along the diagonal direction for a slightly overdoped BSCCO with $T_c = 91$ K (OD 91K)³² and for $\text{La}_{2-x}\text{Sr}_x\text{CuO}_4$ with $x = 0.03$ (Ref.¹⁹). The energy scale for BSCCO is shifted down by $\Delta_D = 8.0$ meV. The solid vertical lines (27 meV, 45 meV, 61 meV) mark the energies of the pronounced phonon peaks in the electron-phonon spectral density ${}^2\text{F}(!)$ that is determined from the MEM procedure¹⁹. The dashed vertical line indicates the energy of a pronounced phonon peak (75 meV) in the superconducting LSCO with $x = 0.07$.

Here we will demonstrate that the fine coupling structures also appear in the earlier high-resolution ARPES data of a slightly overdoped BSCCO with $T_c = 91$ K (OD 91K)³². Fig. 3 shows the real part of electron self-energy along the diagonal direction for the OD 91K sample. In the same figure, we also plot the real part of electron self-energy along the diagonal direction for $\text{La}_{2-x}\text{Sr}_x\text{CuO}_4$ (LSCO) with $x = 0.03$. We can clearly see the fine structures in the raw data of both LSCO and BSCCO. The solid vertical lines mark the energies of the pronounced phonon peaks (27 meV, 45 meV, 61 meV) in the electron-phonon spectral density ${}^2\text{F}(!)$ that is determined from the MEM procedure¹⁹. The dashed vertical line indicates the energy of a pronounced phonon peak (75 meV) in the superconducting LSCO with $x = 0.07$. In order for the fine structures in the self-energy of BSCCO to be aligned with those for LSCO, the energy scale for BSCCO has to be shifted down by $\Delta_D = 8.0$ meV. This suggests that the superconducting gap along

the diagonal direction is not zero. This is consistent with an extended wave gap symmetry that has a finite gap of about 10 meV along the diagonal direction²⁴. The magnitude of Δ_D surely depends on impurities and disorder, so it may vary from samples to samples.

It is interesting to note that the coupling feature at 75 meV is invisible in the deeply underdoped LSCO ($x = 0.03$), but becomes pronounced in the superconducting LSCO ($x = 0.07$) and in BSCCO (OD 91K). This is consistent with the neutron experiments that clearly demonstrate that the coupling to the 75 meV half-breathing mode increases with increasing doping¹⁰. Nevertheless, the electron-phonon coupling constant for this mode is still small (< 0.2) due to a high phonon energy. This implies that this mode alone cannot cause high-temperature superconductivity, in contrast with the claim by Lanzara et al.¹⁷. In fact, the low energy phonon modes below 30 meV along the diagonal direction in LSCO ($x = 0.03$) contribute a large electron-phonon coupling constant (about 0.8).

V. STRONG ELECTRON-PHONON COUPLING FEATURES ALONG THE ANTINODAL DIRECTION

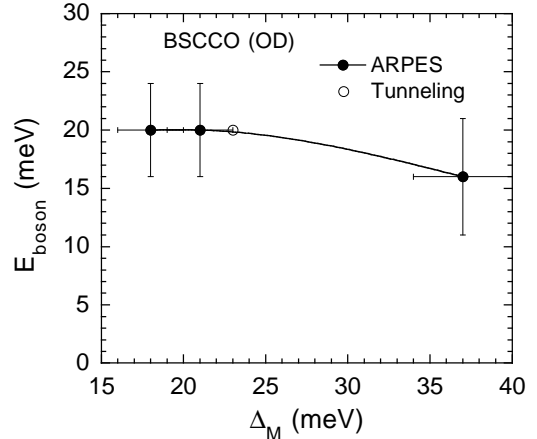


FIG. 4. The boson energy as a function of the antinodal gap Δ_M for several overdoped BSCCO. The boson energy extracted from ARPES (Ref.³³) is calculated according to $E_{\text{boson}} = E_{\text{kink}} - \Delta_M$, where E_{kink} is the kink energy in the band dispersion. One data point (open circle) is from the tunneling data (see Fig. 5).

The electron self-energy effect along the antinodal direction has been studied for several BSCCO crystals (OD 91K, OD 71K, and OD 58K)³³. The kink feature in the band dispersion in the antinodal direction is much stronger than that along the diagonal direction. This indicates a much stronger electron-boson coupling. One of the puzzling issues is that the averaged energy of the

boson modes shifts to a much lower energy (about 20 meV)³³. Fig. 4 shows the boson energy as a function of the antinodal gap M for several overdoped BSCCO. The boson energy is calculated according to $E_{\text{boson}} = E_{\text{kink}} - M$, where E_{kink} is the kink energy in the band dispersion. Since the antinodal gap M was found to be very close to the peak energy in the energy distribution curve (EDC)³⁴, one can simply take M being equal to the EDC peak energy. One can see that the boson energy is about 20 meV for heavily overdoped BSCCO and about 16 meV for nearly optimally doped BSCCO. The strong coupling feature at about 20 meV agrees with the electron-boson spectral density $^2F(\omega)$ deduced from a break-junction spectrum, as shown in Fig. 5. The spectral density clearly shows strong coupling features at about 20 meV, 35 meV, 60 meV, and 72 meV. In particular, the coupling to phonon modes near 20 meV is strongly enhanced (the coupling constant for the 20 meV phonon peak is about 2.6). This unusual enhancement is possible if the extended van Hove singularity is about 20 meV below the Fermi level and the electron-phonon matrix element for the 20 meV phonon modes has a maximum around $q = 0$, where q is the phonon wavevector. The large density of states at the van Hove singularity (20 meV below the Fermi level) and strong Fermi surface nesting along the antinodal direction greatly enhance the phase space available for 20 meV small- q phonons to scatter quasiparticles from the states near the antinodal regime to the extended saddle points. The first principle calculation indeed shows that unusual long-range Madelung-like interactions lead to very large matrix elements especially for zone center modes that are related to vibrations of cations (e.g., La, Sr, Ba, Ca)³⁶. The phonon energies for the vibrations of the cations are between 15 meV to 25 meV.

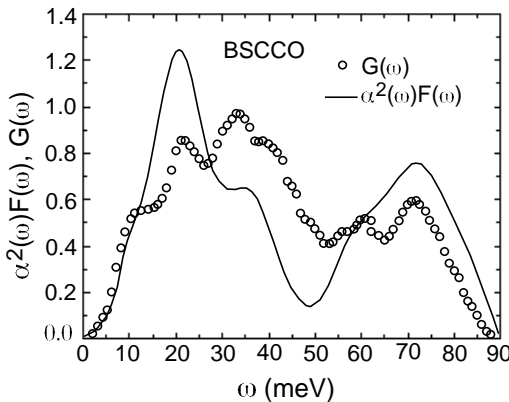


FIG. 5. The electron-phonon spectral density $^2F(\omega)$ for a slightly overdoped $\text{Bi}_2\text{Sr}_2\text{CaCu}_2\text{O}_{8+y}$ (BSCCO) crystal, which was deduced from an SIS break-junction spectrum³⁵.

Now we further show that a strong coupling feature in optical data, which was previously explained as due to a strong coupling between electrons and the mag-

netic resonance mode^{37,38}, is actually consistent with a strong electron-phonon coupling at a phonon energy of about 20 meV. It is known that the electron-phonon spectral density $^2F(\omega)$ can be obtained through inversion of optical data. Marsiglio et al.³⁹ introduced a dimensionless function $W(\omega)$ which is defined as the second derivative of the normal state optical scattering rate $^1(\omega) = (\frac{2}{\omega_p^2} = 4) \times ^1(\omega)$ multiplied by frequency ω . Here ω_p is the bare plasma frequency and $^1(\omega)$ the normal state optical conductivity. Specifically,

$$W(\omega) = \frac{1}{2} \frac{d^2}{d\omega^2} \frac{1}{(\omega)} \quad (5)$$

which follows directly from experiment. Marsiglio et al.³⁹ made the very important observation that within the phonon range $W(\omega) \propto ^2F(\omega)$.

In the superconducting state, a phonon mode that is strongly coupled to electrons will appear at an energy of $2(E_F) + \omega_{\text{ph}}$ (where ω_{ph} is the phonon energy), that is, the energies of the phonon structures shift up by the pair-breaking energy $2(E_F)$ ⁴⁰. Because the 20 meV phonon modes are much more strongly coupled to the states near the antinodal regime and because there is a large quasi-particle density of states at the maximum gap edge, there must be a maximum at $2M + \omega_{\text{ph}}$ in $W(\omega)$. For slightly overdoped BSCCO with $T_c = 90$ K, $M = 26.0(5)$ meV (Ref.^{41,24}), so we should expect a maximum in $W(\omega)$ to be at about 72 meV. This is in quantitative agreement with the result shown in Fig. 6.

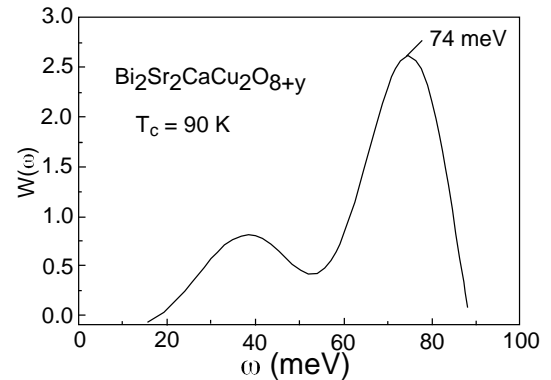


FIG. 6. The optically determined electron-boson spectral density $W(\omega)$ for a slightly overdoped BSCCO crystal with $T_c = 90$ K. After³⁸.

Recently, Devreux et al. have calculated the electron-phonon interactions for the oxygen buckling mode (B_{1g}) and the in-plane half-breathing mode²³. They find that the 40 meV B_{1g} mode couples strongly to electronic states near the antinodal regime. They use an electron-phonon matrix element that is suitable only for $\text{YBa}_2\text{Cu}_3\text{O}_7$ where a large buckling distortion occurs.

For other cuprates, the CuO_2 plane is at and the buckling effect is negligible. Raman data have indeed shown that the coupling constant of the B_{1g} mode in BSCCO is more than one order of magnitude smaller than that in YBCO (Ref.⁴²). Even for YBCO, the coupling constant of this mode was deduced to be about 0.05 from the Raman data⁴², in agreement with the earlier first principle calculation⁴³. Moreover, if this 40 meV phonon were strongly coupled to the electronic states near the antinodal regime, one would expect a maximum in W (!) to occur at about 92 meV in slightly overdoped BSCCO with $T_c = 90$ K. This is in total disagreement with experiment (see Fig. 6).

Previously, the energy of the maximum in W (!) was claimed to be in quantitative agreement with the theoretical prediction based on the strong coupling between electrons and the magnetic resonance mode^{37,38}. Later on, more rigorous theoretical approach⁴⁴ shows that the maximum in W (!) should occur at about $E_M + E_r$ rather than at $E_M + E_r$, where E_r is the magnetic resonance energy. For BSCCO with $T_c = 90$ K, $E_r = 43$ meV, so we should expect a maximum in W (!) to occur at about 95 meV, in disagreement with experiment (see Fig. 6).

The strong electron-phonon coupling feature at about 20 meV is also consistent with the energy distribution curves obtained from ARPES. For a conventional strong-coupling superconductor (e.g., Pb), a dip feature in the single-particle density of states can be clearly seen in the superconducting state. The dip feature appears near $E_M + E_c$, where E_c is the phonon cut-off energy³¹. From Fig. 5, one can see that the cut-off energy for the 20 meV phonon peak is about 40 meV, i.e., $E_c \approx 40$ meV. Since the intensity of EDC is proportional to the single-particle spectral weight, the dip feature should appear in EDC at $E_M + E_c$. Because E_M is close to the EDC peak energy along the antinodal direction, the separation energy between the peak and dip in the EDC should be close to $E_c \approx 40$ meV, in agreement with experiment¹⁵.

V. STRONG COUPLING BETWEEN ELECTRONS AND CU-O CHARGE-TRANSFER EXCITATION.

In addition to strong electron-phonon interactions, there is a pronounced coupling feature at an energy of about 2 eV in the optical reflectance data^{45,46}. In Fig. 7, we plot the superconducting to normal-state reflectance ratio, R_s/R_N for $(\text{BiPb})_2\text{Sr}_2\text{Ca}_2\text{Cu}_3\text{O}_{10}$. It is clear that a strong coupling feature appears at about 2 eV. A similar strong coupling feature was also seen in YBCO, $T_{23}\text{Ba}_2\text{Ca}_2\text{Cu}_3\text{O}_{10}$, and $T_{23}\text{Ba}_2\text{Ca}_1\text{Cu}_2\text{O}_8$ (Ref.⁴⁶). Both the temperature and energy dependence of the optical structure can be well described within Eliashberg theory with an electron-boson coupling constant of 0.30–0.35 (Ref.⁴⁶). Because the energy scale of

this bosonic excitation is similar to the Cu-O charge transfer gap, it is likely that this high-energy bosonic mode corresponds to the Cu-O charge transfer excitation. A recent calculation based on three-band Hubbard model has indeed shown that the high energy Cu-O charge fluctuation can lead to a significant attractive interaction between conduction electrons and that the pairing symmetry is of extended s-wave (A_{1g})⁴⁷. The extended s-wave pairing symmetry is consistent with the conclusion²⁴ drawn from the comprehensive data analyses on nearly all the experiments that are used to test the gap symmetry.

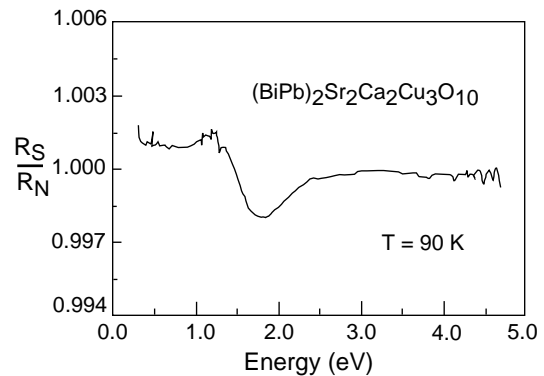


FIG. 7. The superconducting to normal-state reflectance ratio, R_s/R_N for $(\text{BiPb})_2\text{Sr}_2\text{Ca}_2\text{Cu}_3\text{O}_{10}$ ($T_c = 105$ K). After⁴⁶.

VII. PAIRING MECHANISM

In two of our previous papers^{15,16}, we have proposed the pairing mechanism for optimally doped and overdoped cuprates. The long-range Fröhlich-type electron-phonon interaction and the short-range interaction of electrons with high-energy phonons lead to the formation of polarons. These interactions along with the coupling of electrons to the high-energy electronic excitations produce a negative value for the effective Coulomb pseudopotential. The polarons are bounded into the Cooper pairs due to the negative and additional attractive interaction caused by the retarded electron-phonon interaction with the 20 meV phonon modes. The problem could then be solved within Eliashberg equations with an effective electron-phonon spectral density for the low-energy phonons and a negative Coulomb pseudopotential produced by the high-energy phonons and other high-energy bosonic excitations of purely electronic origin. Within this simplified approach, we are able to consistently explain the observed negligible isotope effect on T_c , substantial isotope effect on the supercarrier mass, large reduced energy gap, and high T_c value.

In this modified strong-coupling model, the effective

electron-phonon coupling constant ϵ_p for the low-energy phonons is enhanced by a factor of $f_p = \exp(g^2)$. Here $g^2 = A/\omega_H$, A is a constant, and ω_H is the frequency of the high-energy phonon mode. The value of g^2 can be evaluated from the mid-infrared optical conductivity which exhibits a maximum at $E_m \approx 0.12$ eV for optimally doped BSCCO⁴⁸ and LSCO²⁶. With $E_m = 0.12$ eV, $\hbar\omega_H = 75$ m eV, we find $g^2 = E_m/(2\hbar\omega_H) = 0.8$, leading to $f_p = 2.2$.

From the spectral density shown in Fig. 5, we can extract the effective electron-phonon coupling constant ϵ_p for the low-energy phonon mode, that is, $\epsilon_p \approx 2.6$. If there were no polaronic mass enhancement, the coupling constant contributed from the low-energy phonons would be $2.6/f_p = 1.2$. With $\epsilon = 0.1$ and $\epsilon_p = 1.2$, we calculate $T_c = 18$ K according to a T_c formula⁴⁹

$$k_B T_c = 0.25h \frac{p}{\epsilon_p} \left\langle \epsilon^2 \right\rangle \left[\exp(2\epsilon_{eff}) - 1 \right]^{1/2}; \quad (6)$$

where

$$\epsilon_{eff} = (\epsilon_p - \epsilon) = [1 + 2\epsilon + \epsilon_p t(\epsilon_p)]; \quad (7)$$

The function $t(\epsilon_p)$ is plotted in Fig. 2 of Ref.⁴⁹. In the present case, $h \left\langle \epsilon^2 \right\rangle$ is contributed only from the low-energy phonons and equal to 20 m eV. Therefore, without the polaronic effect, T_c would not be higher than 20 K. On the other hand, with the polaronic effect, $\epsilon_p = 2.6$ and ϵ may be close to zero, leading to a T_c of about 54 K. Thus the polaronic effect enhances T_c significantly, but electron-phonon coupling alone cannot explain superconductivity above 100 K in optimally doped cuprates.

Now we consider two cut-off Lorentzian peaks in electron-boson spectral density: one at 20 m eV due to the low-energy phonon modes and another at 2.1 eV due to the high-energy Cu-O charge transfer excitation. We assume that the attractive interaction due to the high-energy phonon modes makes ϵ close to zero. The optical reflectance data show that the coupling constant ϵ_c for the high-energy boson mode (2.1 eV) is about 0.30 in $(\text{BiPb})_2\text{Sr}_2\text{Ca}_2\text{Cu}_3\text{O}_{10}$ with $T_c \approx 105$ K (Ref.⁴⁶). One can estimate T_c using the approximate analytic expression derived by Allen and Dynes³¹:

$$k_B T_c = \frac{\hbar\omega_H}{12} \exp \left[\frac{1.04(1 + \epsilon)}{(1 + 0.62\epsilon)} \right]; \quad (8)$$

This formula is almost precise for $\epsilon < 1.5$, nearly independent of the details of the spectral density³¹. This can explain why the calculated T_c from the analytic expression in Ref.⁴⁶ is in good agreement with that calculated using the full finite-temperature Eliashberg equations because the coupling constant used in Ref.⁴⁶ is 1.37–1.49. For $\epsilon = 3.0$, the calculated T_c from the analytic expression can be underestimated by 15–35% (Ref.³¹). Thus, the calculated T_c from the analytic expression is a lower limit in the strong coupling regime. From the coupling

constants ($\epsilon_p = 2.6$ and $\epsilon_c = 0.30$), and the mode energies, we can readily find that $\hbar\omega_H \approx 32$ m eV. Substituting $\epsilon = 0$, $\hbar\omega_H = 32$ m eV, and $\epsilon_c = 2.9$ into Eq. 8, we obtain $T_c = 76$ K. If we consider that the analytic expression underestimates T_c by 15–35%, then the theoretically predicted T_c from the two bosonic modes should be 90–103 K, in good agreement with the measured value (105 K). We are underway to evaluate T_c by directly solving the Eliashberg equations.

V III. CONCLUSION

We have determined the polaron binding energy E_p for undoped parent cuprates from the unconventional oxygen-isotope effect on the antiferromagnetic ordering temperature (T_N). The deduced value (about 1.0 eV) of E_p is in quantitative agreement with that estimated from independent optical data and that estimated theoretically from the measured dielectric constants. The polaron-binding energy should be large enough to overcome the intersite Coulomb interaction to form intersite bipolarons in deeply underdoped cuprates, in agreement with theory and experiment^{21,15}. The substantial oxygen-isotope effect on the in-plane supercarrier mass observed in optimally doped cuprates suggests that polarons are bounded into the Cooper pairs. The bipolaron picture may be irrelevant for optimally doped cuprates because the superconducting transition is of BCS-like. We also identify the phonon modes that are strongly coupled to conduction electrons from the angle-resolved photoemission spectroscopy (ARPES), tunneling spectra, and optical data. We consistently show a very strong electron-phonon coupling feature at a phonon energy of about 20 m eV along the antinodal direction. On the other hand, the coupling to the 20 m eV phonon mode becomes weaker towards the diagonal direction so that the coupling features at higher phonon energies become more pronounced. We further show that high-temperature superconductivity in cuprates is caused by strong electron-phonon coupling, polaronic effect, and significant coupling with 2 eV Cu-O charge transfer excitation.

¹ J. G. Bednorz and K. A. Müller, Z. Phys. B 64, 189 (1986).

² R. J. Cava, B. Batlogg, R. B. van Dover, D. W. Murphy, S. Sunshine, T. Siegrist, J. P. Renema, E. A. Rietman, S. Zahurak, and G. P. Espinosa, Phys. Rev. Lett. 58, 1676 (1987).

³ B. Batlogg, R. J. Cava, A. Jayaraman, R. B. van Dover, G.

¹ A. Kourouklis, S. Sunshine, D. W. Murphy, L. W. Rupp, H. S. Chen, A. White, K. T. Short, A. M. Mugee, and E. A. Rietman, *Phys. Rev. Lett.* **58**, 2333 (1987).

² L. C. Boume, M. F. Crommie, A. Zettl, H. zur Loye, S. W. Keller, K. L. Leary, A. M. Stacy, K. J. Chang, M. L. Cohen, and D. E. M. Orris, *Phys. Rev. Lett.*, **58**, 2337 (1987).

³ G. M. Zhao, K. K. Singh, and D. E. M. Orris, *Phys. Rev. B* **50**, 4112 (1994).

⁴ G. M. Zhao and D. E. M. Orris, *Phys. Rev. B* **51**, 16487R (1995).

⁵ G. M. Zhao, K. K. Singh, A. P. B. Sinha, and D. E. M. Orris, *Phys. Rev. B* **52**, 6840 (1995).

⁶ G. M. Zhao, M. B. Hunt, H. Keller, and K. A. Muller, *Nature* (London) **385**, 236 (1997).

⁷ G. M. Zhao, K. K. Conder, H. Keller, and K. A. Muller, *J. Phys.: Condens. Matter*, **10**, 9055 (1998).

⁸ R. J. McQueeney, Y. Petrov, T. Egami, M. Yethiraj, G. Shirane, and Y. Endoh, *Phys. Rev. Lett.* **82**, 628 (1999).

⁹ A. Lanzara, G. M. Zhao, N. L. Saini, A. Bianconi, K. Conder, H. Keller, and K. A. Muller, *J. Phys.: Condens. Matter* **11**, L541 (1999).

¹⁰ A. Shengelaya, G. M. Zhao, C. M. Aegerter, K. Conder, I. M. Savic, and H. Keller, *Phys. Rev. Lett.* **83**, 5142 (1999).

¹¹ J. Hofer, K. Conder, T. Sasagawa, G. M. Zhao, M. Willemin, H. Keller, and K. Kishio, *Phys. Rev. Lett.* **84**, 4192 (2000).

¹² G. M. Zhao, H. Keller, K. Conder, *J. Phys.: Condens. Matter*, **13**, R569 (2001).

¹³ G. M. Zhao, *Phil. Mag. B* **81**, 1335 (2001).

¹⁴ G. M. Zhao, V. Kirtikar, and D. E. M. Orris, *Phys. Rev. B* **63**, 220506R (2001).

¹⁵ A. Lanzara et al., *Nature* (London) **412**, 510 (2001).

¹⁶ R. Khasanov et al., *Phys. Rev. Lett.* **92**, 057602 (2004).

¹⁷ X. J. Zhou et al., *cond-mat/0405130*.

¹⁸ G. M. Zhao, K. Conder, H. Keller, and K. A. Muller, *Nature* (London) **381**, 676 (1996).

¹⁹ A. S. Alexandrov and N. F. Mott, *Polarons and Bipolarons* (World Scientific, Singapore, 1995).

²⁰ Z.-X. Shen, A. Lanzara, and N. Nagaosa, *cond-mat/0102244*.

²¹ T. P. Devereaux, T. Cuk, Z.-X. Shen, and N. Nagaosa, *cond-mat/0403766*.

²² G. M. Zhao, *Phys. Rev. B* **64**, 024503 (2001); G. M. Zhao, *cond-mat/0302566* (to be published in *Phil. Mag. B*); G. M. Zhao, *cond-mat/0305483* (to be published in *Phil. Mag. B*).

²³ B. H. Brandow, *Phys. Rev. B* **65**, 054503 (2002).

²⁴ X. X. Bian and P. C. Eklund, *Phys. Rev. Lett.* **70**, 2625 (1993).

²⁵ A. S. Alexandrov and A. M. Bratkovsky, *J. Phys.: Condens. Matter* **11**, L531 (1999).

²⁶ T. Thio et al., *Phys. Rev. B* **38**, 905 (1988).

²⁷ J. H. Cho, F. C. Chou, and D. C. Johnston, *Phys. Rev. Lett.* **70**, 222 (1993).

²⁸ I. Eremeev, O. Kameev, and M. V. Eremeev, *Phys. Rev. B* **69**, 094517 (2004).

²⁹ J. P. Carbotte, *Rev. Mod. Phys.* **62**, 1027 (1990).

³⁰ P. D. Johnson, T. Valla, A. V. Fedorov, Z. Yusof, B. O. Wills, Q. Li, A. R. Moodenbaugh, G. D. Gu, N. Koshizuka, C. Kondziora, Sha Jian, and D. G. Hinks, *Phys. Rev. Lett.* **87**, 177007 (2001).

³¹ A. D. Gromko, A. V. Fedorov, Y.-D. Chuang, J. D. Koralik, Y. A. Iura, Y. Yamaguchi, K. Oka, Yoichi Ando, and D. S. Dossau, *Phys. Rev. B* **68**, 174520 (2003).

³² H. Ding et al., *Phys. Rev. Lett.* **74**, 2784 (1995).

³³ R. S. Gonnelli, G. A. Ummarino, and V. A. Stepanov, *Physica C* **275**, 162 (1997).

³⁴ W. E. Pickett, R. E. Cohen, and H. Krakauer, *Phys. Rev. Lett.* **67**, 228 (1991).

³⁵ J. P. Carbotte, E. Schachinger, and D. N. Basov, *Nature* (London) **401**, 354 (1999).

³⁶ E. Schachinger and J. P. Carbotte, *Phys. Rev. B*, **62**, 9054 (2000).

³⁷ F. M. Marsiglio, T. Startseva, and J. P. Carbotte, *Physics Lett. A* **245**, 172 (1998).

³⁸ J. Orenstein, *Nature* (London) **401**, 333 (1999).

³⁹ V. M. Krasnov, A. Yurgens, D. Winkler, P. Delsing, and T. Claeson, *Phys. Rev. Lett.* **84**, 5860 (2000).

⁴⁰ M. Opele et al., *Phys. Rev. B* **60**, 9836 (1999).

⁴¹ C. O. Rodriguez, A. I. Liechtenstein, I. I. Mazin, O. Jepen, O. K. Anderson, M. methfessel, *Phys. Rev. B* **42**, 2692 (1990).

⁴² A. Abanov, A. V. Chubukov, and J. Schmalian, *Phys. Rev. B* **63**, 180510R (2001).

⁴³ M. J. Holcomb, J. P. Colman, and W. A. Little, *Phys. Rev. Lett.* **73**, 2360 (1994).

⁴⁴ M. J. Holcomb, C. L. Perry, J. P. Colman, and W. A. Little, *Phys. Rev. B* **53**, 6734 (1996).

⁴⁵ M. Gulacs and R. J. Chan, *J. Supercond.* **14**, 651 (2001), and private communication with M. Gulacs.

⁴⁶ M. A. Quijada, D. B. Tanner, R. J. Kelley, M. Onellion, H. Berger, and G. Margaritondo, *Phys. Rev. B* **60**, 14917 (1999).

⁴⁷ V. Z. Kresin, *Phys. Lett. A* **122**, 434 (1987).